

# Mid-Wave HgCdTe FPA Based on P on N Technology: HOT Recent Developments. NETD: Dark Current and 1/f Noise Considerations

A. KERLAIN,<sup>1,3</sup> A. BRUNNER,<sup>1</sup> D. SAM-GIAO,<sup>1</sup> N. PÉRE-LAPERNE,<sup>1</sup>  
L. RUBALDO,<sup>1</sup> V. DESTEFANIS,<sup>1</sup> F. ROCHETTE,<sup>2</sup> and C. CERVERA<sup>2</sup>

1.—SOFRADIR - Development and Production Center, Actipole - 364 Route de Valence, CS - 10021, 38113 Veurey-Voroize, France. 2.—CEA, LETI, MINATEC Campus, 38054 Grenoble, France. 3.—e-mail: alexandre.kerlain@sofradir.com

For high operating temperature applications, variation of noise equivalent differential temperature (NETD or NEDT) with temperature is the most relevant figure of merit. NETD(T) models with and without taking into account systemic 1/f noise contribution are presented and compared to recent developments made on P on N technology at Sofradir and CEA-LETI. We show that for mature middle wave infrared HgCdTe technology, no 1/f noise contribution up to 220 K is measured and the focal plane array operation is only limited by the mean performance value degradation, not by an increase of defects.

**Key words:** HgCdTe, FPA, MWIR, NETD, 1/f noise

## INTRODUCTION

Most current developments efforts in infrared (IR)-module technology are concentrated on reducing the size, weight and power (SWaP), all of these being key requirements, for instance, for night vision goggles, miniature Unmanned Aerial Vehicles, Thermal Weapon Sights, or more generally all IR systems that require more (performance) for less (volume and price).

The key driver for power consumption of cooled systems is the operating temperature of the focal plane array (FPA). Increasing the temperature of operation ( $T_{\text{FPA}}$ ) is then the priority for most IR detector manufacturers. This field is generally referenced as high operating temperature (HOT) technologies. Today, several solutions are competing, essentially: InAsSb xBn,<sup>1</sup> extrinsic doped HgCdTe P on N<sup>2</sup> and N on P structure.<sup>3</sup> Potentially PiN HgCdTe structure can also respond to tomorrow's HOT requirements.<sup>4</sup> For most applications, users' requests are in the medium wavelength infrared (MWIR) bands. HgCdTe technologies provide solutions for so-called red middle wave

(MW) band (with cut-off wavelength  $\lambda_c = 5.2 \mu\text{m}$ ) and blue MW band ( $\lambda_c = 4.2 \mu\text{m}$ ), whereas available xBn technology is only in the blue MW band due to the fixed ternary InAsSb composition matching the GaSb substrate lattice parameter.

This paper discusses ongoing developments and results on HOT detector for SWaP systems, focusing on NEDT performances with temperature. We present here results from P on N technology developed in the DEFIR laboratory (joint laboratory Sofradir-CEA). The P on N technology is based on Indium N-type doped HgCdTe LPE on CdZnTe substrate. P+ planar diodes are made by Arsenic implantation. Indium doping concentration are in the  $10^{15} \text{ cm}^{-3}$  range ( $\geq 1 \times 10^{15} \text{ cm}^{-3}$ ). Dark current is diffusion limited and follows Rule07.<sup>2</sup>

## NETD(T) WITH NO LOW FREQUENCY NOISE

For FPAs, The most relevant figures of merit is the noise equivalent differential temperature (NETD or NEDT). In most IR detectors, the generated photocurrent is integrated (during the integration time  $T_{\text{int}}$ ) in a capacitance with a carrier well capacity ( $N_w$ ). NETD corresponds to the minimum detectable temperature difference. It is calculated with consideration that the minimum differential

temperature (or detectable flux) equals the root mean square (RMS) voltage value at the integration capacitance node, when only shot noise is present.

A full development of the calculation can be found in Kinch, 2014.<sup>4</sup> In the case of a constant well fill (i.e.,  $N_w = \text{constant}$ , assumption kept in this paper) the NETD becomes:

$$NE\Delta T = \frac{1}{\sqrt{N_w C \eta_{cs}}} \left( 1 + \frac{J_d}{J_\Phi} \right) \quad (1)$$

where  $C$  is the scene contrast through the optic,  $J_d$  is the dark current surface density,  $J_\Phi$  is the input flux surface density and  $\eta_{cs}$  is the coldfield efficiency. The impact of degradation of the coldfield efficiency with temperature is developed in Kinch, 2014,<sup>4</sup> but is shown to be negligible for temperatures  $< 180$  K. Note that in the shot noise limitation case discussed here, the current noise is proportional to  $\sqrt{(J_d + J_\Phi)}$ .

Providing that there is no NETD defect in the FPA (i.e., operability at least  $> 99.5\%$ ), the maximum  $T_{\text{FPA}}$  is reached when NETD equals the maximum NETD value acceptable for the system (typ 30 mK for cooled IR detectors). In today's FPAs for  $\frac{J_d}{J_\Phi} \ll 1$ , a typical value of 15–20 mK can be obtained with a reasonable integration time of 10 ms.<sup>4</sup> In this case, the maximum  $T_{\text{FPA}}$  corresponds roughly to the background limited IR photodetection temperature ( $T_{\text{BLIP}}$ ), usually defined when  $J_d = J_\Phi$ . IR FPA manufacturers usually use more conservative temperatures (i.e.,  $T_{\text{FPA}} < T_{\text{BLIP}}$ ), mainly due to the increase of defect when increasing temperature or due to the need for lower NETD. Indeed, several papers show that before being degraded by the mean value of the NETD, maximum  $T_{\text{FPA}}$  is in the first place limited by a degradation of the operability below 99.5%.<sup>1–6</sup>

In Eq. 1, the most important factor is the dark current to signal current ratio.

In the most usual case, HOT detectors dark current is diffusion limited in the pseudo-neutral absorbing layer. In that case,  $J_d$  the dark current becomes<sup>4</sup>:

$$J_d = \frac{q \cdot n_i^2 \cdot t}{N \cdot \tau} \quad (2)$$

$q$  is the elementary charge,  $N$  is the majority doping in the neutral absorbing layer,  $\tau$  is the minority carrier lifetime,  $t$  is the absorbing layer thickness,  $n_i$  is the intrinsic carrier density, with  $n_i^2 \sim \exp\left(\frac{-E_g(T)}{kT}\right)$  and  $E_g$  the energy band gap of the absorbing layer. Note that Eq. 2 is valid for  $N \gg n_i$  (which is true for  $T \leq 220$  K, with cut-off wavelength  $\lambda$  discussed in this paper).

Rule07 is a semi-empirical expression of the 2007 state of the art dark current in HgCdTe P on N Teledyne technology. For  $\lambda_c > 4.6 \mu\text{m}$  and for HOT, it corresponds to the dark current expected from

Auger 1 theory ( $\tau = \tau_{A1}$  and  $N = 10^{15} \text{ cm}^{-3}$  in Eq. 2).<sup>7</sup> Eight years later, Rule07 is still representative of the state of the art photodetector for FPA HOT applications.

The input flux  $J_\Phi$  depends on the quantum efficiency  $\eta$  (in mature photodetector  $\eta$  is  $> 0.7$ ), the system field of view (i.e. F number) and the cut-off wavelength of the absorbing layer ( $J_\Phi$  will decrease with increasing  $E_g$ ).

Thus, the temperature of operation  $T_{\text{FPA}}$  can be increase in several ways:

*Increasing the band gap* with reduction of the cut-off wavelength, in particular from the red MW band ( $\lambda_c = 5.2 \mu\text{m}$ ) to the blue MW band ( $\lambda_c = 4.2 \mu\text{m}$  typ), leads both  $J_\Phi$  and  $J_d$  to be reduced. However, the higher dark current reduction compensates for the input signal loss, as described in Fig. 1, where expected NETD with rule07 for blue and red bands are plotted from Eq. 1. (Note that in that case,  $N_w$  were adjusted for normalizing minimum NETD to 20 mK).

*Dark current reduction* at constant band gap; the relevant figure of merit for dark current is the  $N \cdot \tau$  product (Eq. 1). For constant doping  $N$ , using Auger7 limited P type pseudo-neutral absorbing layer (extrinsic N on P HgCdTe) instead of shorter Auger1 N type lifetime  $\tau$  (extrinsic N on P HgCdTe) can potentially increase the  $T_{\text{FPA}}$ . This is described in Fig. 2; assuming an Auger7 to Auger 1 ratio of  $\gamma = 10$ . A +20 K, an increase of  $T_{\text{FPA}}$  can then be expected.

*Increase the input signal* at constant well fill; the increase of input signal (Field of view or F#) will automatically increase  $T_{\text{FPA}}$ . In that case, we can estimate a +5 K for each decrease of F number from 4 to 3 to 2, as shown in Fig. 3.

## NETD(T): LOW FREQUENCY NOISE CONSIDERATION

The NETD is degraded by the increase of ‘‘systemic’’ low frequency noise with temperature. The

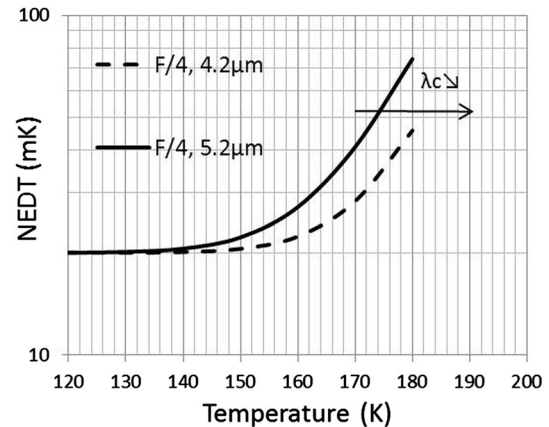


Fig. 1. NETD expected from Eq. 1 with rule07 dark current for 4.2  $\mu\text{m}$  and 5.2  $\mu\text{m}$  cut-off wavelength ( $N_w$  were adjusted for normalizing minimum NETD to 20 mK).

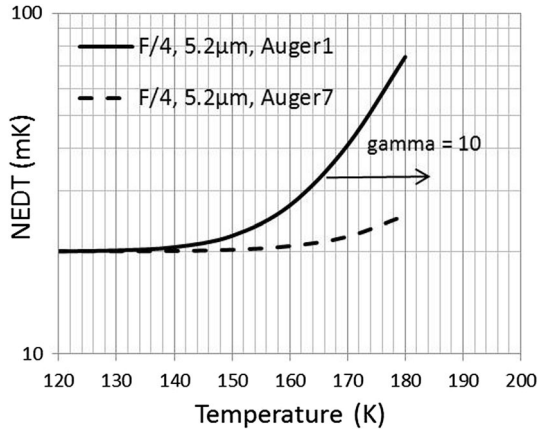


Fig. 2. NETD expected from Eq. 1 with rule07 (Auger1 limited,  $N_d = 1 \times 10^{15} \text{ cm}^{-3}$ ) dark current compared with Auger7 ( $N_a = 1 \times 10^{15} \text{ cm}^{-3}$ ) for  $5.2 \mu\text{m}$  cut-off wavelength (with the assumption that  $\gamma = 10$ ).

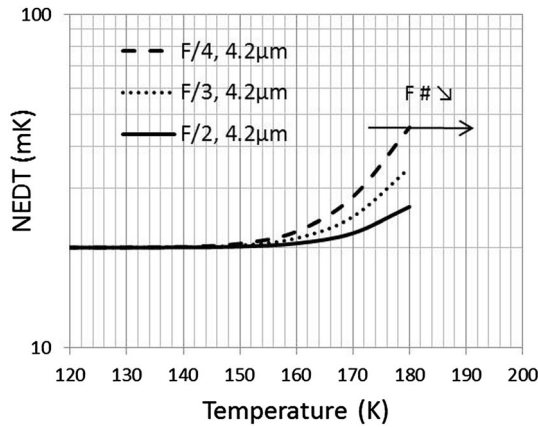


Fig. 3. NETD expected from Eq. 1 with rule07 dark current for  $4.2 \mu\text{m}$  cut-off wavelength (with different input signals).

systemic noise appears for  $T > T_{1/f}$ , when the contribution of the low frequency noise is no longer negligible compared to the minimum photodetector noise floor (i.e., shot noise).

The term “systemic” means that all diodes of the FPA will present additional low frequency noise. In that case,

$$\text{NETD} = F \cdot \frac{1}{\sqrt{N_w} C \eta_{cs}} \left( 1 + \frac{J_d}{J_\Phi} \right) \quad (3)$$

$F > 1$  is the excess noise factor due to low frequency noise. The maximum temperature of operation will be degraded to a temperature  $T_{\text{FPA}} < T_{1/f} < T_{\text{BLIP}}$ .

### Low Frequency Noise in HgCdTe Photodetectors

Several papers have studied low frequency noise in HgCdTe photodiode.<sup>3,8-10</sup> Low frequency noise has a  $1/f$  current power spectrum density usually proportional to the dark current.<sup>8,10</sup> When the dark

current is in a diffusion regime, the noise current is proportional to  $n_i^2$  ( $\sim \exp(E_g/kT)$ ), whereas in the case of a generation recombination regime in the depletion layer, the noise becomes proportional to  $n_i$  ( $\sim \exp(E_g/2 kT)$ ). In the rest of this paper, we focus on the diffusion regime.

First,  $1/f$  noise investigations were made by Tobin et al.,<sup>8</sup> who proposed a simple expression of the noise current density in HgCdTe photodiodes:

$$S_I^{1/2} = \frac{\alpha \cdot I_d^\beta}{\sqrt{f}} \quad (4)$$

$I_d$  is the diode dark current,  $\alpha = 1 \times 10^{-3}$  and  $\beta = 1$ .

With  $A$  as the diode area, in this paper we introduce the factor  $\alpha_s = \alpha \cdot A$  ( $\text{cm}^2$ ), which is the Tobin’s  $\alpha$  coefficient times the diode area, and then:

$$S_I^{1/2} = \frac{\alpha \cdot J_d \cdot A}{\sqrt{f}} = \frac{\alpha_s \cdot J_d}{\sqrt{f}} \quad (5)$$

The low frequency noise behavior of the detector is then fully described by the  $\alpha_s$  coefficient, which depends on the technology and diode design. We can define a noise figure  $i_n$  as the noise in  $\text{A}/\text{Hz}^{1/2}$  measured at 1 Hz normalized to the square root of the diode area as:

$$i_n = \frac{\alpha_s \cdot J_d}{\sqrt{A}} \quad (6)$$

In Kinch’s photodiode  $1/f$  noise model,<sup>10</sup> the noise current spectral density is given by:

$$S_I^{1/2} = \frac{J_v}{N} \sqrt{\frac{N_T \cdot A_{\text{eff}}}{f}} \quad (7)$$

where  $J_v$  is the dark current in the volume affected by surface charge fluctuation,  $N$  is the majority carrier concentration in this volume, and  $N_T$  the surface trap density.  $A_{\text{eff}}$  is a diode effective surface impacted by the  $1/f$  noise. This effective surface is a function of diode design and  $\leq A$ . Simplifying the assumption  $J_v = J_d/t$  ( $t$ , the thickness of the absorbing layer):

$$i_n = \frac{1}{t \cdot N} \sqrt{N_T \cdot \frac{A_{\text{eff}}}{A}} \cdot J_d \quad (8)$$

Combining Eqs. 6 and 8 leads to equivalent expressions for  $i_n$  from<sup>8</sup> and<sup>10</sup> with:

$$\alpha \cdot A = \alpha_s = \frac{1}{t} \frac{\sqrt{N_T}}{N} \cdot \sqrt{A_{\text{eff}}} \quad (9)$$

Note that  $\alpha_s$  depends on the pixel pitch through  $\sqrt{A_{\text{eff}}}$ . The noise figure  $i_n$  is proportional to the dark current surface density.

### Low Frequency Noise in HgCdTe Photodetectors: Impact on NETD

In the case of  $1/f$  noise, the additional current noise can be calculated as follows:

$$I_{\text{rms}}\left(\frac{1}{f}\right) = \sqrt{\frac{1}{2T_{\text{int}} \int \frac{\alpha_s^2 J_d^2}{f} df}} \quad (10)$$

with  $T_t$ , total time of measurement.

Equation 1 can be rearranged including this addition noise, giving an expression of the excess noise factor at the output capacitance node:

$$F = \sqrt{1 + \alpha_s^2 \cdot \frac{N_w \cdot \ln\left(\frac{T_t}{2T_{\text{int}}}\right)}{\left(1 + \frac{J_d}{J_q}\right)^2}} \quad (11)$$

The term  $N_w \cdot \ln\left(\frac{T_t}{2T_{\text{int}}}\right)$  is a dimensionless constant, and is typically equal to a few  $N_w$ .

By convention and as discussed in the previous chapter, with no  $1/f$  noise, the maximum temperature of operation with  $1/f$  noise ( $T_{1/f}$ ) is reached when  $F \cdot \left(1 + \frac{J_d}{J_q}\right) = 2$  with  $T_{\text{FPA}} < T_{1/f} < T_{\text{BLIP}}$ .

Figure 4 illustrates  $1/f$  noise for different  $\alpha_s$  values, for a dark current that follows rule07 with  $\lambda_c = 5.2 \mu\text{m}$  @80 K (Fig. 4a), and their impact on the NETD (Fig. 4b) estimated from Eqs. 3 and 11.  $1/f$  noise is estimated for a  $15 \mu\text{m}$  pitch FPA @ 150 K. NETD degradation becomes non-negligible for  $\alpha_s > 10^{-3}$ .

### Low Frequency Noise in HgCdTe Photodetectors: Recent Measurements

Figure 5a shows the low frequency current noise spectral density measured on  $15 \mu\text{m}$  pitch confined diodes test devices (MWIR blue) in dark condition. Figure 5b is  $i_n$  versus dark current density. Present results are compared with DRS from<sup>9,10</sup>; these data show that the transition between shot noise limited behavior ( $i_n$  proportional to the square root of the dark current) and  $1/f$  limited case ( $i_n$  proportional to the dark current as expected from Eqs. 6 and 8) is at  $220 \text{ K} < T_{1/f} < 250 \text{ K}$ . In the  $1/f$  regime  $i_n(J_d)$ , slope is equal to  $2 \cdot 10^{-8} \text{ cm}$  (i.e.,  $\alpha_s = 1 \times 10^{-5} \text{ cm}^2$ ), and is slightly below DRS HgCdTe reference. To our knowledge, this is the state of the art noise figure for  $15 \mu\text{m}$  pitch IR-FPA.

As  $T_{1/f} > T_{\text{BLIP}}$  (estimated around 170 K, see Fig. 1), there is no  $1/f$  noise impact on NETD(T) on these devices.

### NETD(T): COMPARISON WITH EXPERIMENTAL DATA

Data are measured on  $15 \mu\text{m}$  pitch  $640 \times 512$  formats FPA for red and blue MWIR bands. Experimental dark currents used in the model are

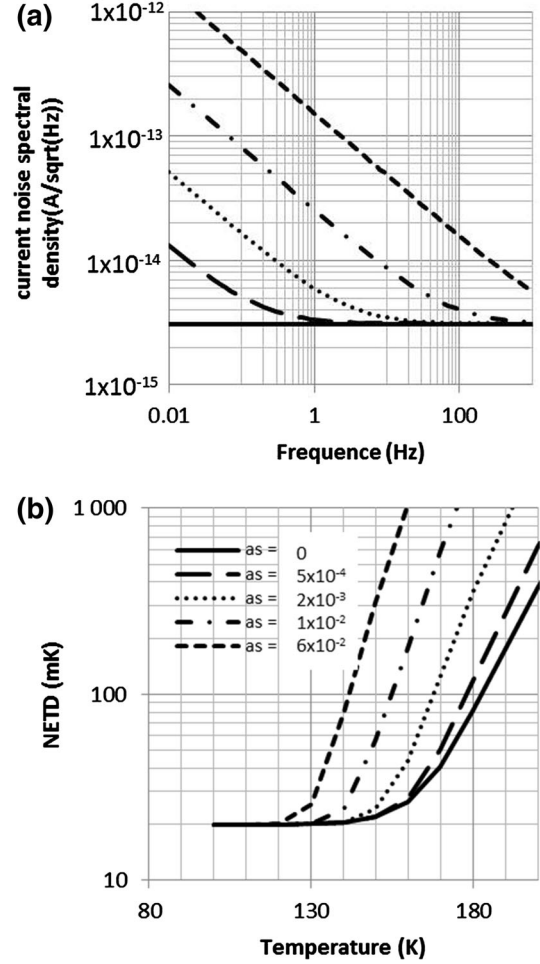


Fig. 4. (a)  $1/f$  noise for different  $\alpha_s$  values, for a dark current that follows rule07 with  $L_c = 5.2 \mu\text{m}$  @80 K. (b) impact of  $1/f$  noise (a) on NETD (T) from Eqs. 3 and 11.

extracted from the same devices. We show here the mean NETD value measured on the FPA.

### 1/f Noise Contribution: Red Band Example

Figure 6 shows experimental data compared with Eq. 3. We show that noisy FPA (A, from older technology) can be modeled with  $\alpha_s = 7 \times 10^{-3} \text{ cm}^2$ ,  $J_d$  corresponding to rule07 (confirmed by dark measurement on same devices). However, optimized technology from CEA-LETI shows no contribution to  $1/f$  noise ( $\alpha_s = 0$ , i.e.  $F = 1$ ).

### No 1/f Noise Contribution: Blue Band Example

In Fig. 7, NETD of 2 FPAs with different dark currents around rule07 ( $0.4 \times \text{Rule07}$  and  $2.5 \times \text{Rule07}$ ) are plotted. Experimental data fit Eq. 1 for both devices; thus, no  $1/f$  noise contribution is observed up to 220 K. As expected, the same value of NETD is reached at higher  $T_{\text{FPA}}$  with reduced dark current. In both cases,  $T_{\text{BLIP}} > 160 \text{ K}$ . Maximum  $T_{\text{FPA}}$  will finally depend on the FPA operability. This is discussed in the next chapter.



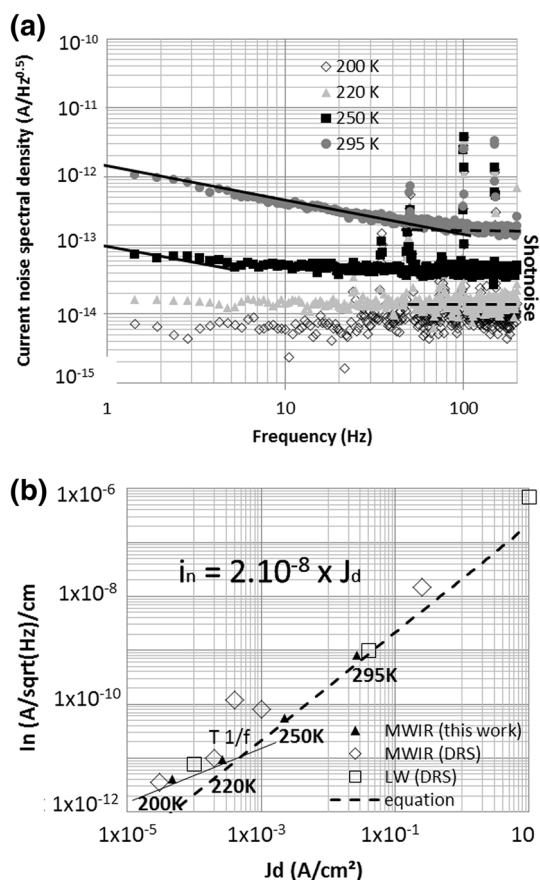


Fig. 5. (a) Spectral density of low frequency current noise measured on 15  $\mu\text{m}$  pitch confined diodes test devices (MWIR blue) in dark condition. (b)  $i_n$  versus dark current density. This work is compared with DRS data taken from [9, 10].

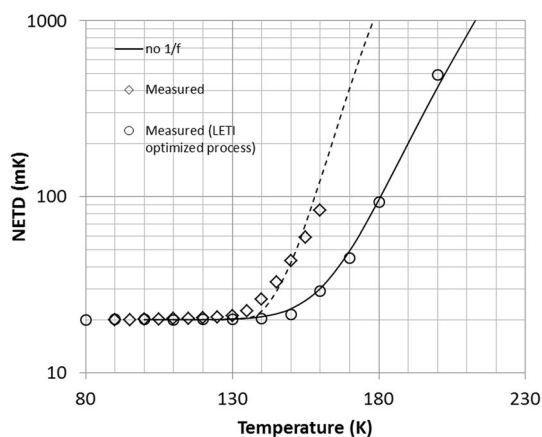


Fig. 6. NETD(T) experimental data compared with Eq. 3. FPA A is modeled with  $a_s = 7 \times 10^{-3} \text{ cm}^2$ ,  $I_{\text{dark}}$  rule07, FPA B with  $a_s = 7 \times 10^{-3} \text{ cm}^2$ ,  $I_{\text{dark}}$  rule07.

### NETD(T) OPERABILITY

The ideal case for FPA operation is when the limitation comes from performance mean value degradation (mean value limited FPA operation) rather than by defect limitation (defect limited FPA

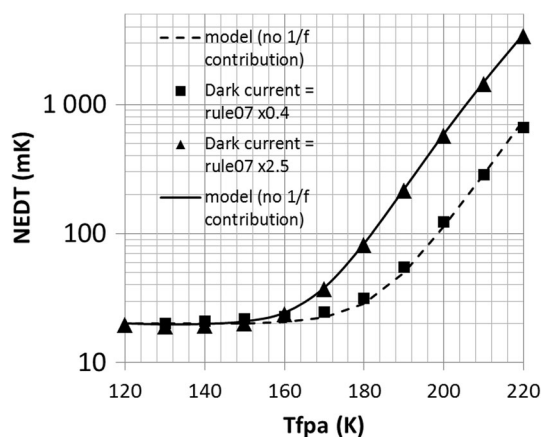


Fig. 7. NETD(T) of 2 FPAs with different dark currents around rule07 ( $0.4 \times \text{Rule07}$  and  $2.5 \times \text{Rule07}$ ). Experimental data fit with Eq. 1.

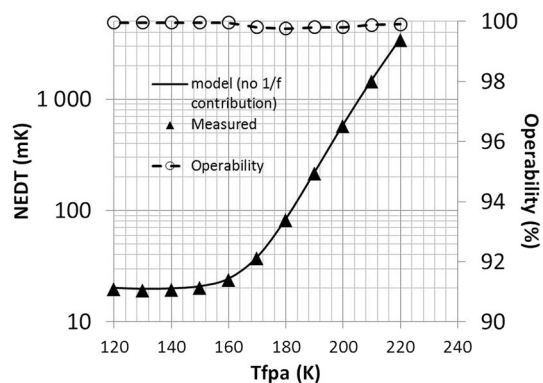


Fig. 8. NETD(T) and operability measured on  $640 \times 512$  15  $\mu\text{m}$  pitch FPA F/4 (MWIR blue band).

operation). However, several papers show that before being degraded by the mean value of the NETD, maximum  $T_{\text{FPA}}$  is in the first place limited by a degradation of the operability below 99.5% [1, 5].

The operability criterion we use at Sofradir is  $\text{NETD} \times 2$ . This means that any pixel with NETD value exceeding two times the mean value is considered as a defect. Pertinence of this criterion is discussed in Cathignol et al. [11]. We show in Fig. 8 that it is indeed possible to have very high operability ( $> 99.8\%$ ) up to 220 K (measured on  $640 \times 512$  15  $\mu\text{m}$  pitch FPA F/4), i.e.,  $T_{1/f} \geq 220$  K. At this temperature, performances are degraded as expected from Eq. 1: the operation of this FPA is limited by the mean value degradation. This result confirms our first estimation from 1/f noise measurement on test diodes (see Fig. 5). The only limitation is that expected from dark current increase with temperature (Eq. 1).

Histograms of RMS noise (or NETD) are plotted for two temperatures: 150 K (Fig. 9) and 220 K (Fig. 10), for the same FPA. Histograms are Gaussian shaped (dashed line) for all temperatures from 120 K to 220 K.

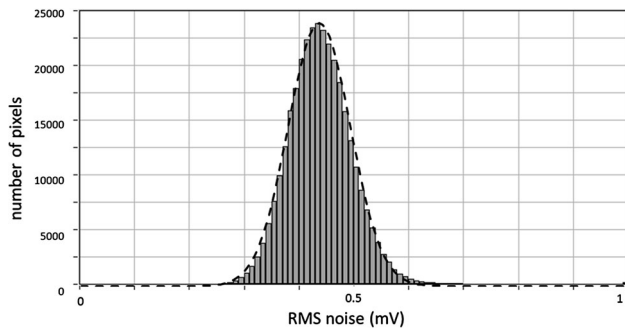


Fig. 9. Histograms of RMS noise measured on  $640 \times 512$   $15 \mu\text{m}$  pitch FPA F/4 (MWIR blue band) at 150 K.

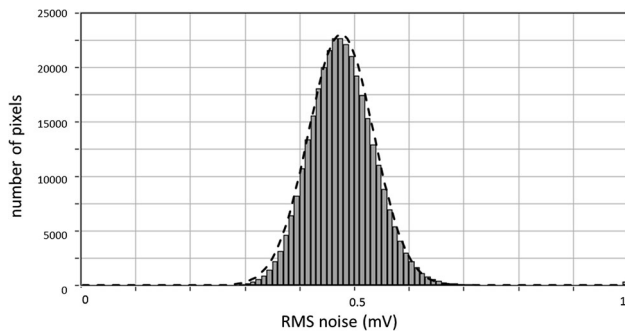


Fig. 10. Histograms of RMS noise measured on  $640 \times 512$   $15 \mu\text{m}$  pitch FPA F/4 (MWIR blue band) at 220 K.

The maximum temperature of operation  $T_{\text{FPA}}$  will only depend on the maximum affordable NETD value for the system; in the case of the FPA presented in Fig. 7, with a 30 mK NETD  $T_{\text{FPA}} = 165$  K.

## CONCLUSIONS

FPA relevant figure of merit (NETD) is modeled with and without taking into account photodetector systemic low frequency noise. These models have been compared to experimental data from HgCdTe Sofradir (MWIR blue) and CEA-LETI FPA (MWIR red). Older devices with low frequency noise show a good concordance with the model developed in this

paper. In more recent technologies, we show that there is no longer  $1/f$  contribution to the degradation of the NETD with temperature up to 220 K. This result was confirmed by direct current noise measurement on test devices, and shows a state of the art noise figure of  $\alpha_s = 1.10^{-5} \text{ cm}^2$ . NETD(T) is only dark current limited (rule07) and perfectly follows NETD expression in Eq. 1. Moreover, we show that for mature HgCdTe technology, defect density is limited to 0.2% up to 220 K in MWIR. This means that the FPA operation is only limited by the mean performance value degradation, not by an increase of defects. These performances allow for temperatures of operation  $T_{\text{FPA}} \geq 160$  K (MWIR blue, F/4).

## ACKNOWLEDGEMENTS

The authors want to thank the people involved in this program: C. Cassillo, L. Dargent and Y. Reibel. The French department of defense is also acknowledged for financial support.

## REFERENCES

1. P.C. Klipstein, Y. Gross, D. Aronov, M. Ben Ezra, E. Berkowicz, Y. Cohen, R. Fraenkel, A. Glozman, S. Grossman, O. Klin, I. Lukomsky, T. Marlowitz, L. Shkedy, I. Shtrichman, N. Snapi, A. Tuito, M. Yassen, and E. Weiss, *Proc. SPIE* (2013). doi:[10.1117/12.2015747](https://doi.org/10.1117/12.2015747).
2. Y. Reibel, R. Taalat, A. Brunner, L. Rubaldo, T. Augéy, A. Kerlain, N. Péré-Laperne, A. Manissadjian, O. Gravrard, P. Castelein, and G. Destéfanis, *Proc. SPIE* (2015). doi:[10.1117/12.2179212](https://doi.org/10.1117/12.2179212).
3. R.L. Strong, M.A. Kinch, and J.M. Armstrong, *Proc. SPIE* (2013). doi:[10.1117/12.2015816](https://doi.org/10.1117/12.2015816).
4. M.A. Kinch, *State-of-the-Art Infrared Detector Technology* (Bellingham: SPIE Press, 2014).
5. P. Knowles, L. Hipwood, L. Pillans, R. Ash, and P. Abbott, *Proc. SPIE* (2011). doi:[10.1117/12.903042](https://doi.org/10.1117/12.903042).
6. H. Lutz, R. Breiter, H. Figgemeier, T. Schallenberg, W. Schirmacher, and R. Wollrab, *Proc. SPIE* (2014). doi:[10.1117/12.2050427](https://doi.org/10.1117/12.2050427).
7. W.E. Tennant, *J. Electron. Mater.* 39, 1030 (2010).
8. S.P. Tobin, S. Iwasa, and T.J. Tredwell, *IEEE Trans. Electron Devices* 27, 43 (1980).
9. W. Hassis, O. Gravrard, J. Rothman, and S. Benahmed, *J. Electron. Mater.* 42, 3288 (2013).
10. M.A. Kinch, C.F. Wan, H. Schaaake, and D. Chandra, *Appl. Phys. Lett.* 94, 193508 (2009).
11. A. Cathignol, G. Vauquelin, A. Brunner, V. Destefanis, L. Rubaldo, M. Maillard, and M. Runtz, *Proc. SPIE* (2015). doi:[10.1117/12.2178034](https://doi.org/10.1117/12.2178034).